



FLUCOME 2009

10th International Conference on Fluid Control, Measurements, and Visualization
August 17–21, 2009, Moscow, Russia

A STUDY ON THE BEHAVIOR OF SHOCK WAVE AND VORTEX RING DISCHARGED FROM A PIPE

S. KITAJIMA¹, J. IWAMOTO² and E. TAMURA³

Corresponding author S. KITAJIMA

ABSTRACT

In this paper, the behavior of shock wave discharged from the pipe end is studied. The shock wave is generated using the shock tube (MO-tube). The flow field while the shock moves downstream is visualized using shadow photography and schlieren photography. The propagation of shock wave and the phenomenon of the occurrence of second vortex ring are examined and discussed.

Keywords: Shock Wave, Shock Tube, Vortex Ring, Underexpanded Jet, Visualization

INTRODUCTION

The shock wave can be found in many flow fields, for example, in the exhaust pipe of a car engine, in the exploded gas of gunpowder, at the leading edge of the wing of the airplane of a supersonic flight, etc. The shock wave is diffracted when it is discharged from the pipe open end (Skews, 1967(part 2); Skews, 1967(part 4)), and at the same time sound is generated. This sound generation is similar to the occurrence of sound from a tunnel which rapid transit railway vehicle produces and from an exhaust system of an engine, thus causing a noise problem. Therefore, the mechanism of noise generation has been much studied so far experimentally and numerically (Endo *et al.*, 2000; Nakayama *et al.*, 2000). When the shock wave is discharged from the pipe, jet forms behind the shock and vortex ring follows along the jet boundary. The behavior of this vortex ring and the jet is interesting, and many numerical studies as well as experimental studies have been carried out (Baird, 1987; Endo and Iwamoto, 2005). It is well-known that the phenomena of diffraction of a shock wave, and the formation of vortex ring and jet are different for different Mach numbers of the shock wave discharged from the pipe. It has been found that at shock Mach number higher than $Ms = 1.34$ another shock forms within the vortex ring with downstream movement of the vortex ring, and at the same time underexpanded jet develops from the pipe exit. Moreover, as the vortex ring moves further downstream, a new vortex ring appears in front of it (Minota, 1998; Ishii, *et al.*, 1999). Minota named it “thin vortex” and Ishii *et al.* (1999) named “second vortex”.

¹ Tokyo Denki University graduate school, 2-2 Kanda-Nishiki-cho, Chiyoda-ku, Tokyo 101-8457,
e-mail: 08gmm06@ms.dendai.ac.jp

² Tokyo Denki University, 2-2 Kanda-Nishiki-cho, Chiyoda-ku, Tokyo 101-8457, e-mail: iwamoto@cck.dendai.ac.jp

³ Tokyo Metropolitan College of Industrial Technology, 8-17-1 Minami-Senju, Arakawa-ku Tokyo 116-0003,
e-mail: ema@acp.metro-cit.ac.jp

In the present study in order to make clear the above-mentioned phenomena the visualization study is conducted, and the results are examined and discussed.

EXPERIMENTAL CONSIDERATION

The experimental apparatus is shown in Fig. 1. For a shock wave generation, a non-diaphragm type shock tube (MO-tube) is used. The shock wave, vortex ring and jet discharged from a pipe are visualized using the shadowgraph and the schlieren methods. Air is used in the low pressure and high-pressure chambers of a shock tube. The moisture and oil are removed from the air compressed by the compressor using dry filter and oil filter. The cleaned air is stored in the high-pressure chamber of a shock tube (MO-tube). The air in the high-pressure chamber is set at a certain pressure, and then, the solenoid valve is opened by pushing a switch. So the high-pressure air moves to the low pressure chamber momentarily, a shock wave being formed in the low pressure chamber. The shock wave passes the sensors 1 and 2 mounted on the pipe at the positions of 500 and 200 mm measured from the exit of the pipe, respectively, and the pressures are recorded on an oscilloscope. The elapsed time for the shock wave to pass between the sensors 1 and 2 is measured by the universal counter. so that the velocity and Mach number of the shock wave are obtained. On the other hand, the sensor 3 mounted diametrically opposite to the sensor 1 can delay the flashing time of a spark arbitrarily by retarder (The duration of flashing is 20-30 nsec.). Accordingly, the flow field can be visualized at various times. The concave mirrors 1 and 2 are of the same specifications. Their diameters are 300 mm and the focal lengths 3000 mm. Each distance between the centerline of the pipe axis and the concave mirrors 1 and 2 is 1900 mm. The low pressure chamber of the shock tube is made of steel, its length being 5625 mm and its internal diameter $D = 41.6$ mm. The round flange is attached to the pipe end whose diameter is 420 mm. The shock Mach number is varied from 1.25 to 1.45 in experiment.

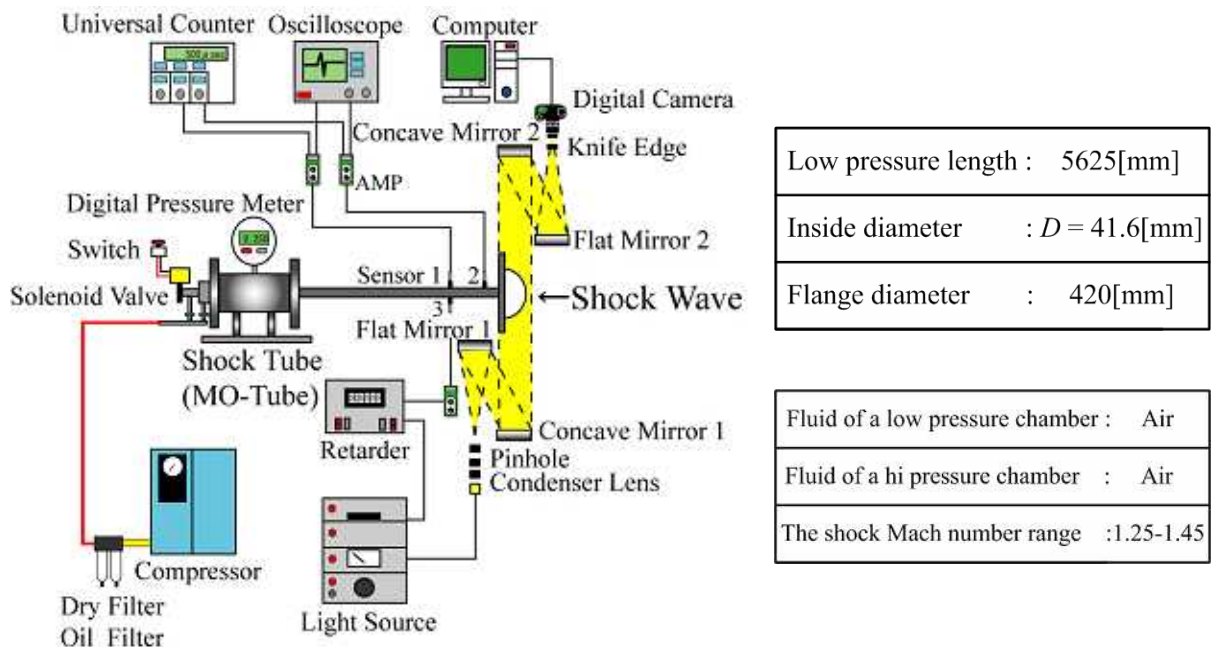


Fig. 1. Experimental Apparatus

(Schlieren method arrangement)

RESULTS AND DISCUSSION

VISUALIZATION OF THE FLOW FIELD

Figures 2 to 4 show the pictures of the visualized flow field at shock Mach numbers $Ms = 1.25$, 1.35 and 1.45 where the shock wave emitted from the shock tube and the vortex ring following it develop with time. The time is measured from the instant when the shock reaches the end of the tube.

Figure 2 shows schlieren and shadowgraph pictures as the flow pattern develops with time for the shock Mach number $Ms = 1.25$. It is seen at time $60\mu\text{sec}$ in Figs. 2(a) and 2(e) that the shock wave is diffracted due to the expansion wave generated at the lip of the open end of the tube, and the vortex ring can also be seen near the lip. The vortex ring grows as it propagates downstream as shown in Figs. 2(b), 2(f), 2(c) and 2(g), and the jet develops and moves downstream with the vortex ring as in Figs. 2(c), (g), 2(d) and 2(h).

The temporal change of flow patterns at $Ms = 1.35$ is shown in Fig. 3. In Figs. 3(b) and 3(f) it is seen that the jet is slightly underexpanded with intercepting shock which is not found in Figs. 2(b) and 2(f). This indicates that the pressure at the tube end is higher than the back pressure. Figs. 3(b), 3(f), 3(c) and 3(g) show discontinuity within the vortex ring which is upward facing shock and which does not appear in Fig. 2. The vortex ring is found to move faster than that for $Ms = 1.25$ in Fig. 2.

Figure 4 represents the photographs of the flow pattern for $Ms = 1.45$. Generally the similar flow patterns are obtained as exhibited in Figs. 2 and 3, except that the underexpanded jet and shock wave newly formed within the vortex ring are more clearly shown. In Figs. 4(c) and 4(g) a tiny vortex ring is visible in front of the shock wave. It is called “second vortex ring” in the present study.

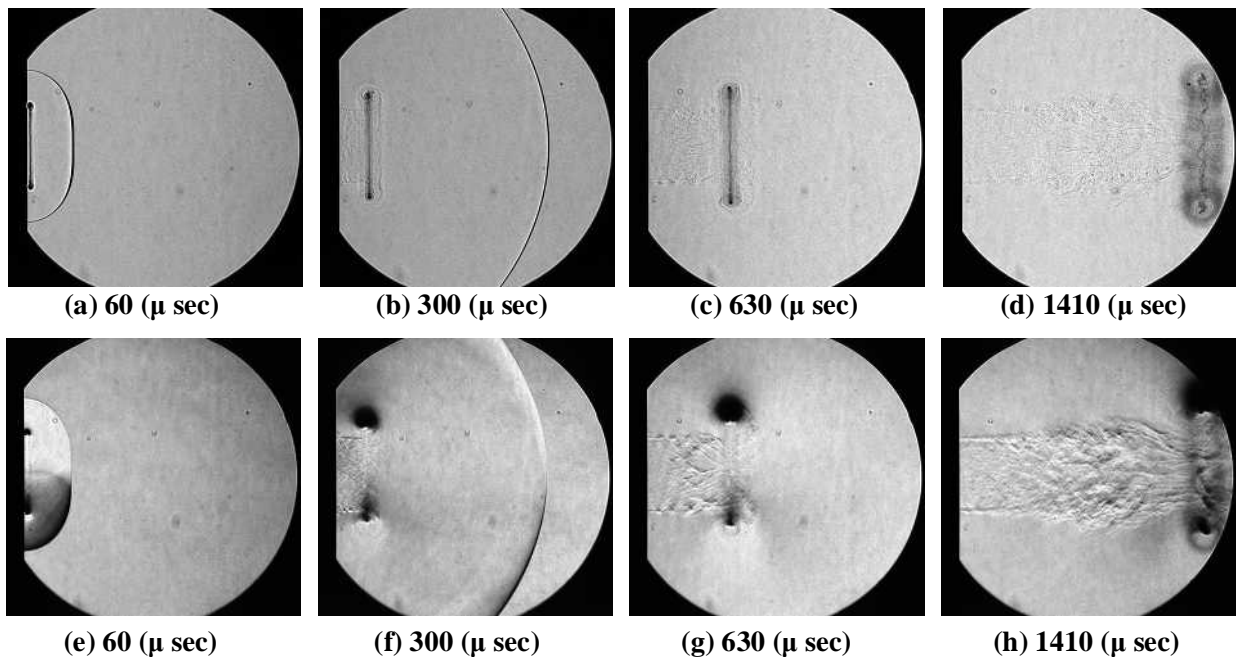


Fig. 2. Visualization Photograph $Ms = 1.25$ (Upper : Shadowgraph, Lower : Schlieren)

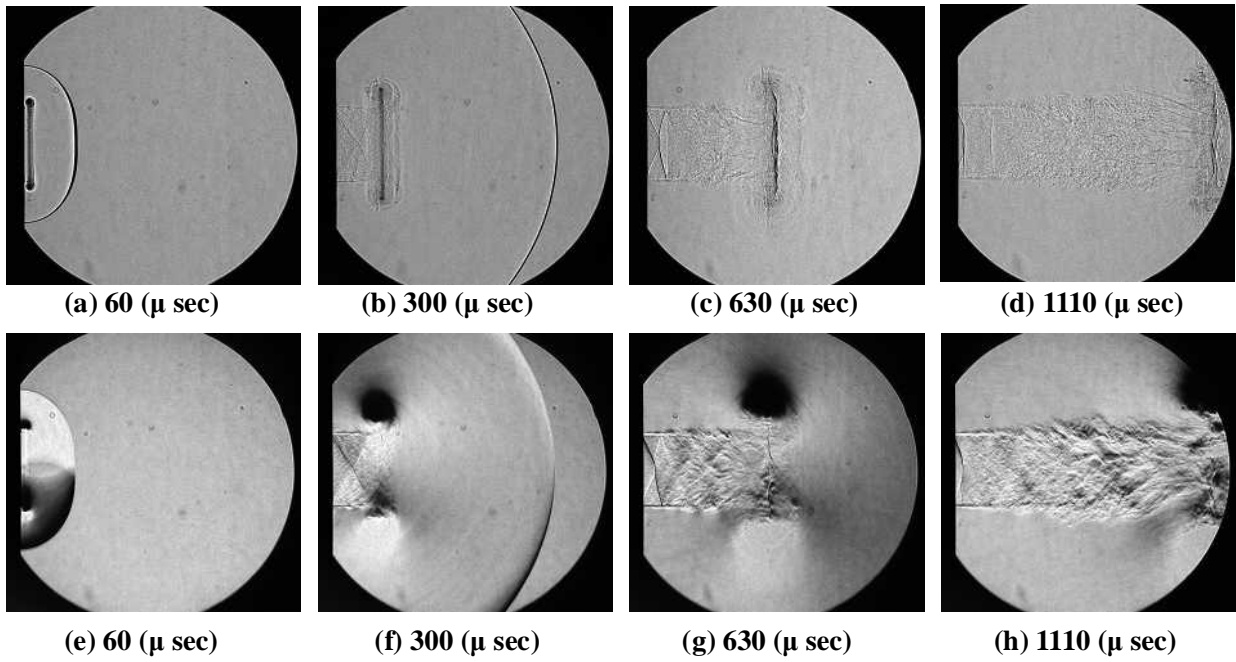


Fig. 3. Visualization Photograph $M_s = 1.35$ (Upper : Shadowgraph, Lower : Schlieren)

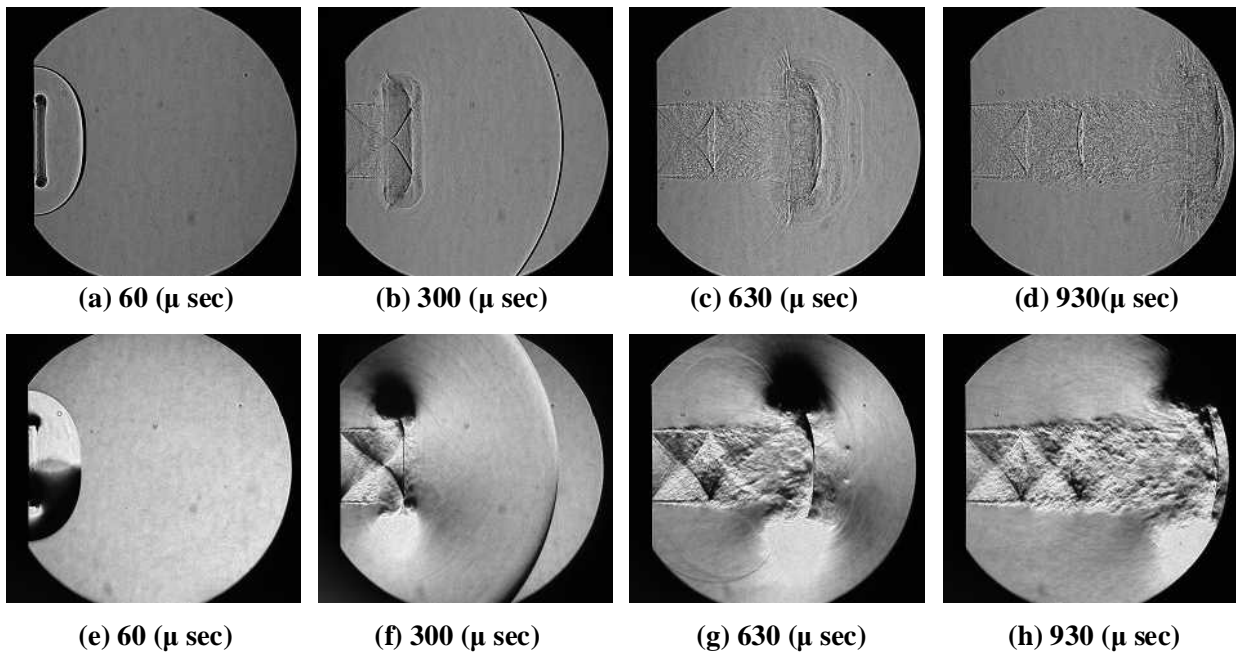


Fig. 4. Visualization Photograph $M_s = 1.45$ (Upper : Shadowgraph, Lower : Schlieren)

DIFFRACTION AND PROPAGATION OF A SHOCK WAVE

Figure 5 illustrates that the shock wave discharged from the pipe diffracts. IT is the normal shock wave, TR is the expansion wave and TC is the diffracted shock wave, where flow Mach number M_2 behind the shock wave is less than unity. In the earlier stage after the shock wave is discharged from the pipe exit, the shock wave is almost normal [(see Fig. 5(a)]. As time elapses, the shock wave is diffracted by interfering with the expansion wave generated at the lip of the pipe. This expansion wave, as it spreads towards the tube axis, interferes with the shock wave. In this process the shock wave is diffracted more and finally it becomes spherical in shape [(see Fig. 5(b))]. As time passes, the shock propagates downstream with constant because the self-similarity is valid in this flow field (Skews, 1967(part 2)).

Figure 6 shows change in the shock wave Mach number with time for different initial shock Mach numbers. The horizontal axis is the time in μ sec measured from the instant when the shock wave reaches the tube exit. The measurement of the shock position is made at the central axis. Immediately after the shock is discharged by the tube, shock wave Mach numbers are almost constant. At about 90 μ sec Mach number decreases suddenly, and then, the Mach numbers of all shock waves gradually approach unity. In the inset in Fig. 6, the times required for each shock wave to become spherical in shape are indicated. It is found that the strength of the shock near the central axis remains constant until it becomes spherical after the discharge of the shock from the tube. The sudden decrease in shock Mach number is due to the fact that the shock wave interferes with the expansion wave at the central axis.

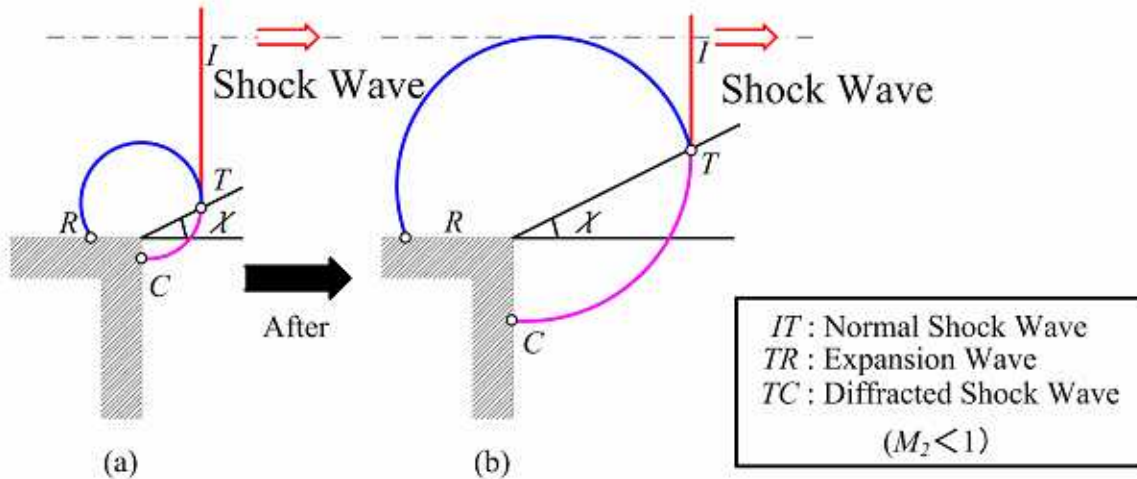


Fig. 5. Shock Wave Diffraction

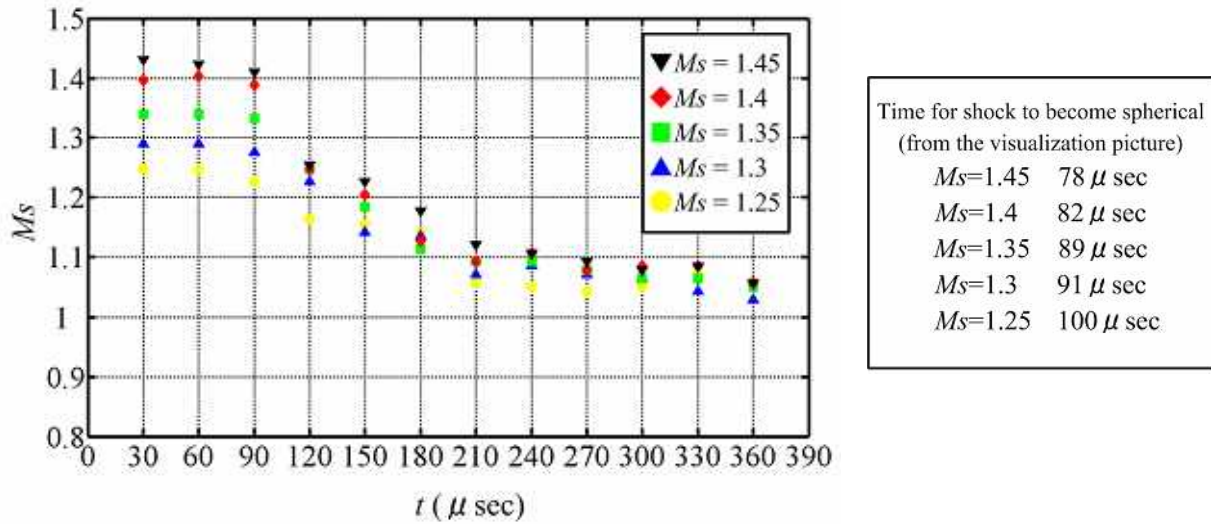


Fig. 6. Shock Wave Propagation

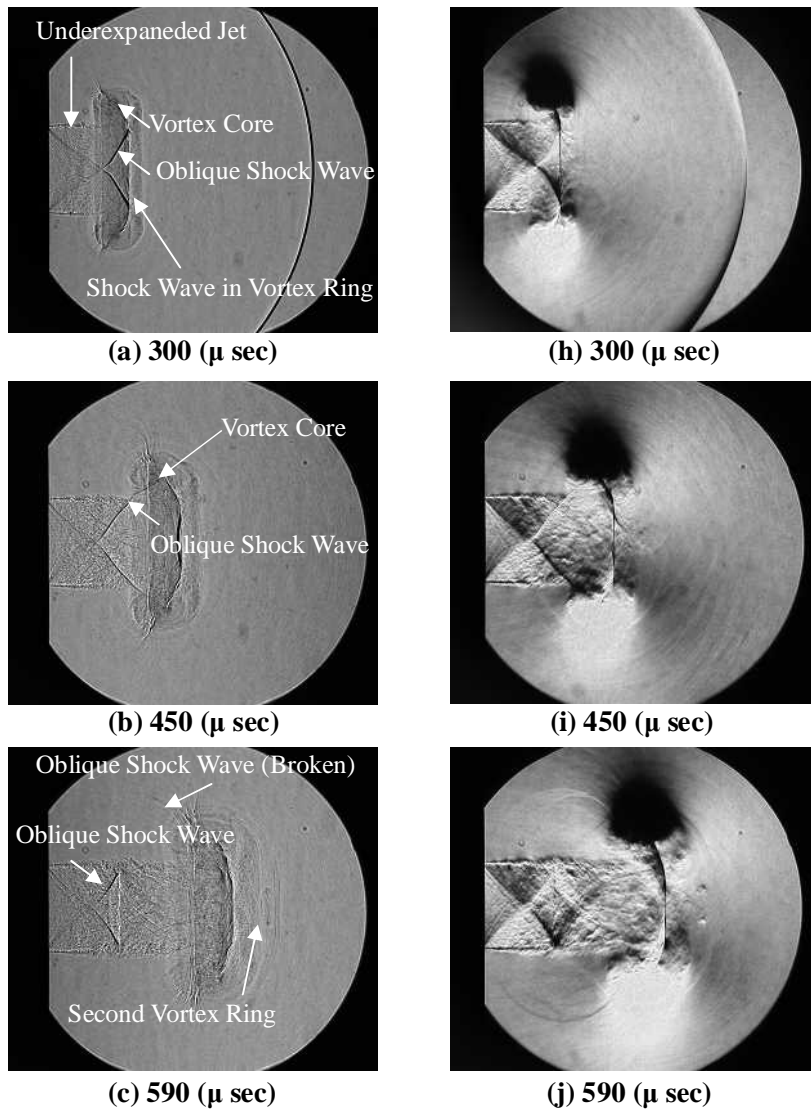
THE SHOCK WAVE IN A VORTEX RING AND THE SECOND VORTEX RING

Figure 7 indicates the shadowgraph and schlieren pictures, where the development of the shock in the vortex ring and the second vortex is shown. The mechanism whereby the shock is formed within the vortex ring is as follows. Immediately after the shock wave is discharged from the tube, the jet forms and the vortex ring is generated on the jet boundary. As the vortex ring moves downstream, the cross-sectional area of the jet passing through the vortex ring decreases, which makes the jet accelerate to sonic speed at the minimum cross-section of the jet. Thus, the jet is very much like the flow through the convergent-divergent nozzle, so that the shock is possible to appear downstream of and near its minimum cross-section (Baird, 1987). The generating mechanism of the shock in a vortex ring is discussed by Endo and Iwamoto, 2005. This shock wave propagates with the vortex ring downstream. As seen in Figs. 7(a), 7(h), 7(b), and 7(i) underexpanded jet follows the shock in the vortex ring. This phenomenon is found to occur when $M_s = 1.35$ and 1.45 . Thus, it is considered that the appearance of the shock in the vortex ring has something to do with the formation of the underexpanded jet.

As shown in Figs. 7(b) and 7(i), the oblique shock wave in the compression region of the jet, after it forms, begins to extend to the vortex core and finally it breaks as can be seen in Figs. 7(c) and 7(j). The broken piece of the oblique shock propagates with the vortex ring, spreading in the surrounding air in an arc with its center near the vortex core. The above phenomena occur when $M_s = 1.4$ and 1.5 , and they are not observed at shock Mach number less than $M_s = 1.35$.

In addition to the above phenomena, in the central area near the jet axis ahead of the vortex ring, the small vortex ring (the second vortex ring) is newly generated as shown in Figs. 7(c) and 7(j). As time elapses, this second vortex ring grows, propagating together with the vortex ring as shown in Figs. 7(d) and 7(k). In the early stage of formation of this vortex, it grows in very stable manner. As it grows further, it becomes gradually unstable as shown in Figs. 7(e) and 7(l). Then, as in Figs. 7(f) and 7(m), the second vortex ring grows radially without moving downstream, starts to cover the vortex ring and finally reaches the jet behind the vortex ring. This change of flow pattern can be indicated in Figs. 7(f) 7(m), 7(g) and 7(n). Subsequently, the second vortex ring interacts with the jet and disappears. This phenomenon occurs at $M_s = 1.4$ and 1.45 .

Figure 8 shows the trace of the second vortex ring at $Ms = 1.4$ and 1.45 . The upper part and the lower part of vortex core (radii) of the second vortex ring are plotted in the figure. The spacing between the neighboring data points at each shock wave Mach number is $30 \mu\text{sec}$. The horizontal and vertical axes are axial and radial distances non-dimensionalized by the internal diameter of the shock tube. Since the second vortex ring becomes unstable at a certain time, the plot in the figure is in the limits where the stable propagation can be seen. The second vortex ring at $Ms = 1.45$ expands in radial direction and breaks more quickly compared with that at $Ms = 1.40$, the behavior of the second vortex ring being much dependent upon the Mach number of the shock wave. And both vortex rings are in good axial symmetry.



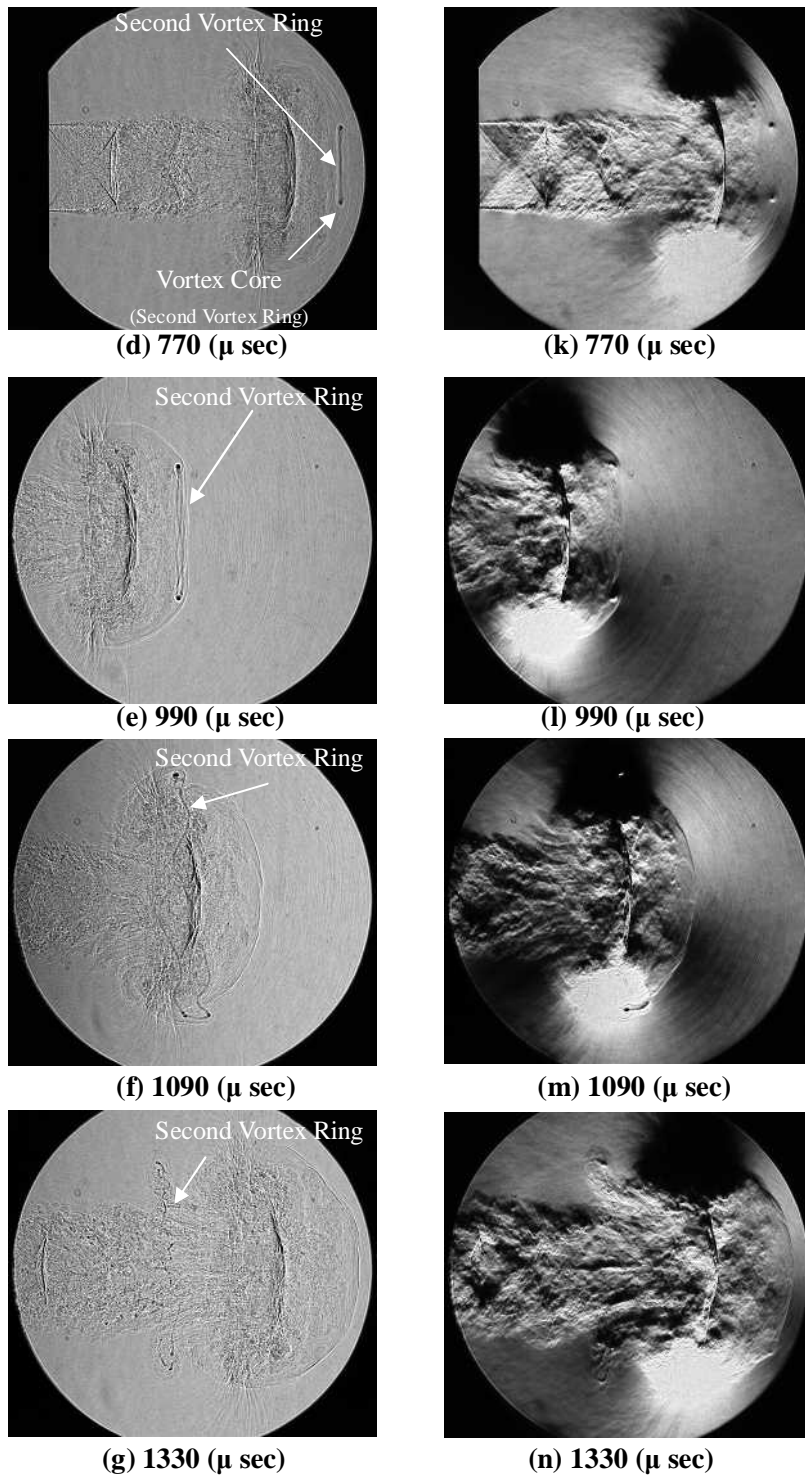


Fig. 7. Shock Wave in a Vortex Ring and Second Vortex Ring

$Ms = 1.45$ (Left : Shadowgraph, Right : Schlieren)

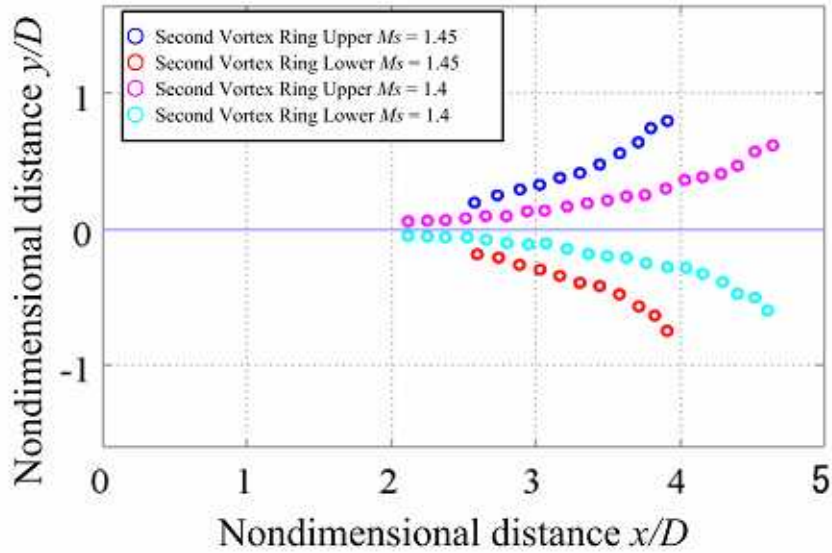


Fig. 8. Second Vortex Ring Vortex Ring Trajectory

UNDEREXPANDED JET

As described above, underexpanded jet is obtained when the pressure at the tube open end is higher than the back pressure, its structure being cellular and consisting of compression and expansion regions. In the present study underexpanded jet occurs at shock Mach number higher than $Ms = 1.35$. Table 1 shows the features of this jet at different shock Mach numbers. The higher the shock Mach number, the longer the maximum length of the first cell and the longer the time needed for the jet to attain the maximum cell length. At $Ms = 1.40$ and 1.45 the oblique shock in the jet extends to the vortex core and at later time it breaks, resulting in the formation of the first cell. For this reason it is considered that it takes more time for jet formation than that at $Ms = 1.35$. The duration of the first cell increases as the shock Mach number becomes high. The duration of the cell at $Ms = 1.35$ is, in particular, much shorter than others. All these data indicate much dependency on the shock Mach number.

Table 1. Underexpanded Jet

Shock Wave Mach Number [Ms]	1.35	1.4	1.45
1st Cell Maximum Length [x/D]	0.51	0.74	0.97
Time to the Maximum Length [μ sec]	380	460	480
Duration of 1st Cell [μ sec]	1720	7210	11290

CONCLUSIONS

The following conclusions are drawn from the experimental study on the behavior of the shock wave emitted from the shock tube and the flow pattern behind it.

- (1) The strength of the shock wave discharged from the pipe decreases as it interferes with the expansion wave. In this study the propagation characteristic of the shock wave is clarified.
- (2) The appearance of the shock wave in the vortex ring and the underexpanded jet are closely related, and these phenomena occur at shock Mach number higher than $M_s = 1.35$.
- (3) Oblique shock which is formed to extend from underexpanded jet to the vortex core breaks at a certain time a shock Mach number higher than $M_s = 1.4$.
- (4) The second vortex ring appears at shock Mach number higher than $M_s = 1.4$, and the trajectory and the limit for its stable movement depend upon the shock Mach number.
- (5) The maximum length of the 1st cell of the underexpanded jet becomes longer and the time needed to attain the maximum length becomes also longer as the shock Mach number is higher.

ACKNOWLEDGMENTS

The experiments described above were made in cooperation with Mr. H. Tsuchiya. The authors would like to thank his assistance.

REFERENCES

- J. P. Baird (1987), "Supersonic vortex rings", Proc. R. Soc. Lond. A **409**, pp. 59-65.
- M. Endo, and J. Iwamoto (2005), "A Study on Shock Wave formed in Unsteady Jet through Vortex Ring", Transactions of JSME (B), **71** (712), 2928-2933 (in Japanese).
- M. Endo, Y. Futagami and J. Iwamoto (2000), "Relation between the flow pattern downstream of duct and the noise", JASE Review 21, pp. 125-132.
- R. Ishii, H. Fujimoto, N. Hatta and Y. Umeda (1999) "Experimental and numerical analysis of circular pulse jets", J. Fluid Mech. Vol. 392, pp. 129-153.
- T. Minota (1998), "Shock/vortex interaction in a flow field behind a shock wave emitted from a shock-tube", Proc. of 2nd Int. Workshop on Shock-Wave/Vortex Interaction, (1998), 2-11.
- H. Nakayama, H. Kashimura, H. D. Kim and T. Setoguchi (2000) "Passive control of impulsive wave discharged from open-end of tube (Reduction of magnitude by means of box with helical vane)", Transactions of JSME (B), **66** (646), 1387-1391 (in Japanese).
- B.W. Skews (1967), "The Shape of a diffracting shock wave", J. Fluid Mech. Vol. 29, part 2, pp. 297-304.
- B.W. Skews (1967), "The perturbed region behind a diffracting shock wave", J. Fluid Mech. Vol. 29, part 4, pp. 705-719.

APPENDIX I. NOTATION

D	Tube internal diameter [mm]
t	Time [μ sec]
	Angle (see Fig. 5) [deg]

M_s	Mach number of a shock wave
M_2	Mach number behind shock wave
x	Axial distance [mm]
y	Radial distance [mm]